Comparison of optimized interferential stimulation using two pairs of electrodes and two arrays of electrodes*

Yu Huang[1] and Abhishek Datta[2]

Abstract— **Interferential stimulation (IFS) or Temporal Interference (TI) has recently generated considerable interest as computational models show that it can focally stimulate deep brain regions with non-invasive transcranial electrical currents [1]. However, the proposed solution in [1] requires two arrays, involving dozens of electrodes in each, to achieve optimal focality in the deep brain regions. Implementation of this approach is usually not feasible in practice due to the limited number of channels and the associated accuracy and precision needed in current stimulation devices. Alternative method [2] focuses on using only two pairs of electrodes as proposed in the conventional IFS approach and searching exhaustively in the parameter space for the optimal montage that maximizes the focality of the modulation at the deep target. Here we compare these two methods in terms of the quality of the solutions (focality versus modulation depth) and the practicality (speed and number of electrodes needed). We then give general guidelines for optimal IFS in practice for future studies.**

I. Introduction

Interferential stimulation (IFS) or Temporal Interference (TI) applies sinusoidal waveforms of similar frequency through two pairs of electrodes [3]. However, un-optimized IFS does not show any significant advantage over conventional high-definition transcranial electrical stimulation [4]. There have been efforts to optimize the focality of IFS [5], [6], [2], but these are limited to two pairs of electrodes as originally proposed by [3]. We recently presented a rigorous framework for optimizing IFS using two arrays of electrodes [1], but results showed that dozens of electrodes are needed to achieve optimal focality, especially for targets in the deep brain regions. In practice, limited number of channels with the requisite accuracy and precision at the IFS frequencies are available in current stimulation hardware options. To make our solution feasible, here we limit the number of electrodes (i.e. channels) and compare that with the recently published method using exhaustive search on two pairs of electrodes [2]. We discuss the pros and cons of each method and provide general guidelines for future practice involving optimized IFS.

II. Methods

Data from three adult male neurologically normal subjects (30, 36 and 46 years old) previously considered [7] were used in this computational study. We named their head models as H1, H2, and H3, respectively. T1-weighted magnetic resonance images (MRI) were acquired from a 3-T MRI scanner with a resolution of 1 mm^3, see [7] for detailed acquisition parameters. To generate the lead field [8], [9] that is needed for targeted IFS, a fully-automated toolbox ROAST was used [10]. With a simple one-line command [11], ROAST generates the lead field for each of these subjects from their T1 MRIs. 72 electrodes following the international 10/10 system [12] were placed on the scalp surface by ROAST in this process.

We first replicated the exhaustive search process for an optimal montage using two pairs of electrodes, as implemented in [2]. The same target location in the deep brain region was selected as in [2], i.e., the head of the right hippocampus. Exhaustive search was performed across: (1) four possible electrodes selected from the 72 placed electrodes on the scalp; (2) three possible ways of pairing in these four electrodes for the two frequencies used in IFS; (3) amplitudes of injected current at one pair of electrodes, in the range of 0.5 mA to 1.5 mA, with a step size of 0.05 mA and the sum across the two pairs of electrodes being 2 mA. See [2] for more details. In total 64,813,770 montages were considered for each target in each head model (1,028,790 possible combinations of 4 electrodes $\times$ 3 possible ways of pairing $\times$ 21 amplitudes of injected current). The optimal montage is the one that achieves maximal ratio of peak modulation depth at the target to that at the non-target region (Eq. 3 in [2]). See [4] for the definition of modulation depth. Note that in our implementation, we computed the modulation depth along the radial direction, i.e., the direction pointing from the target location to the center of the brain (defined as MNI coordinates of [0,0,0]), instead of the modulation depth along the direction of maximal modulation as in [2]. We preferred radial direction as performing another internal search for maximal modulation direction would increase the computational load of the exhaustive search process that is already computationally intensive (takes about 2 days to find one solution).

We then replicated the more rigorous formulation in optimizing the focality of IFS using two arrays of electrodes. We implemented Eq. 18 in [1], with the power constraint on non-target region starting from $P_{max} \times 10^8$ and reducing to $P_{max} \times 10^{-3}$, where P_{max} was obtained from the lead field and specified target location (see [1], [13] for details). This uses most of the electrodes in the full array of 72 electrodes, which is usually not practical as most stimulation devices do not have more than 32 channels. To reduce the electrodes needed in the solution, we only used the top K electrodes

*This work was supported by NIH grant number 75N95020C00024

[1]Y. Huang is with the Department of Radiology, Memorial Sloan Kettering Cancer Center, New York, NY 10065, USA huangy7 at mskcc.org

[2]A. Datta is with Research & Development, Soterix Medical, Inc., New York, NY 10001, USA adatta at soterixmedical.com

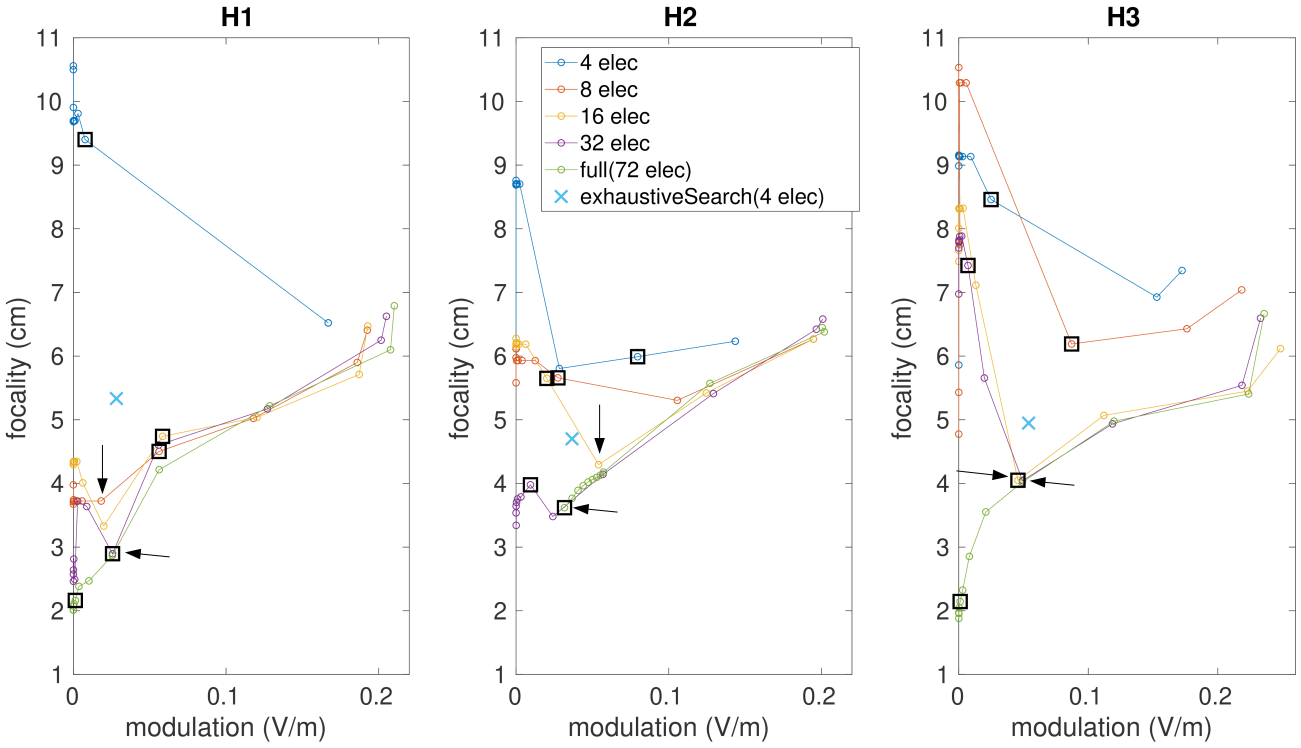

Fig. 1. Relationship between focality (cm) and modulation depth (V/m) across the three subjects considered (H1–H3). Circles on the curves are solutions from rigorous optimization across two arrays of electrodes [1], with different curves representing different numbers of total electrodes used for stimulation under different power constraints. The full array contains 72 electrodes. Blue crosses indicate solutions from exhaustive search using two pairs of electrodes [2]. Black squares on the curves indicate injected current reaches the safety limit of 2 mA. Circles indicated by arrows are visualized in Figure 2.

($K \leq 32$) that receive the most currents. As the solutions can be different corresponding to different levels of the power constraint P_{max} (green curves in Figure 1), we first identified the solution $\mathbf{s}$ that gives the closest modulation depth to the one achieved by the solution from exhaustive search, and then we sorted the absolute values of the injected current in $\mathbf{s}$ for each of the two frequencies and took out the top $K/2$ electrodes for each frequency. Lead field corresponding to these K electrodes ($K/2$ for each frequency) was taken out and re-referenced to the electrode with the smallest absolute value of injected current in these K electrodes. This subset of lead field was used to re-run the same optimization as in Eq. 18 in [1], with the same 12 levels of power constraints mentioned above. The final solution only has up to K electrodes (see Figure 2C).

For each solution, the modulation depth and its focality at the target location were computed. The focality is defined as the cubic-root of the brain volume with modulation depth of at least 50% of the modulation at the target [4]. All computation times (CPU time in Figure 2) reported were measured on a workstation with Intel® Xeon® Silver 4114 CPU at 2.20 GHz.

III. Results

Figure 1 shows the focality–modulation curves for all the solutions for targeting the right hippocampus in the three head models using different methods. Results from the exhaustive search on two pairs of electrodes [2] are shown as blue crosses, and those from the rigorous optimization using two arrays of electrodes [1] are plotted as circles, with different colors representing different numbers of total electrodes used in the montages. Circles are connected assuming linear interpolation. It is clear that the rigorous optimization using full array of 72 electrodes can give solutions that have better focality than the exhaustive search using only two pairs of electrodes under the same level of modulation depth (comparing blue crosses with green curves). The focality decreases as the intensity of modulation increases (green curves), as dictated by the theoretical research [14]. However, as we reduce the electrode numbers in the solutions, the focality–modulation curves are not strictly monotonic, especially if the total injected current is smaller than the safety limit in transcranial stimulation of 2 mA (left of black squares on the purple, orange, red and blue curves). For the three head models, rigorous optimization with $K = 4$ electrodes gives solutions with worse focality compared to that from the exhaustive search (blue curves vs. blue crosses). For H2 and H3, even using $K = 8$ electrodes in the rigorous optimization cannot achieve the same performance in focality as the exhaustive search (red curves vs. blue crosses). This is because with 8 or fewer electrodes, the optimization has difficulty finding the solution that satisfies the objective

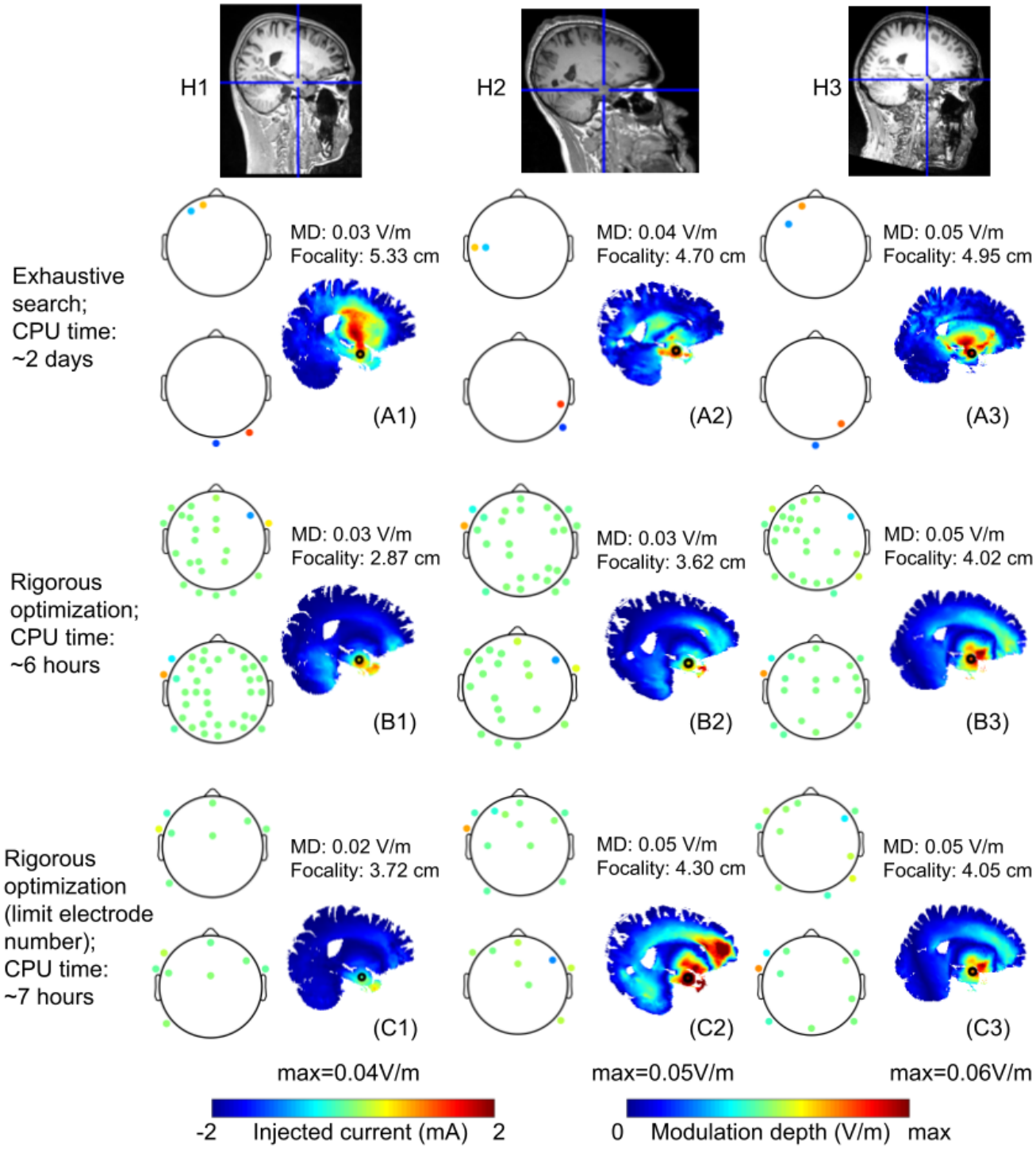

Fig. 2. Exemplary cases of electrode montages and distributions of the modulation depth for the exhaustive search using two pairs of electrodes [2] and the rigorous optimization across two arrays of electrodes [1]. These examples are taken from those data points indicated by arrows and the blue crosses in Figure 1. (A) Exhaustive search; (B) rigorous optimization; (C) rigorous optimization with $K = 8$ electrodes for H1, and $K = 16$ electrodes for H2 and H3. The two topoplots in each panel show the montage for each frequency in the interferential stimulation. CPU time for each method is noted. Focality and modulation depth (MD) for each solution is also indicated in each panel.

function and all the constraints as specified in Eq. 18 in [1]. However, with 16 or more electrodes, we can get much more focal stimulation compared to exhaustive search using only two pairs of electrodes (orange/purple/green curves vs. blue crosses).

Few exemplary cases from Figure 1 (blue crosses, and circles indicated by arrows) are shown in Figure 2 for the three head models. Under approximately the same level of modulation depth (MD), we see in Figure 2 that the rigorous optimization using two full arrays of 72 electrodes gives better focality (2.87 cm, 3.62 cm, 4.02 cm in panels B1–B3) compared to that from the exhaustive search with two pairs of electrodes (5.33 cm, 4.70 cm, 4.95 cm in panels A1–A3). Note that the computation time is also much shorter ($\sim$ 6 hours in rigorous optimization vs. $\sim$ 2 days in exhaustive search). When constraining the number of electrodes in the rigorous optimization, we found that the solution becomes less focal but is still better than that from the exhaustive search. For H1, 8 electrodes can generate more focal solution compared to the exhaustive search while still maintaining approximately the same level of modulation (3.72 cm vs. 5.33 cm, panel C1&A1). For H2 and H3, 13 electrodes are needed to generate a modulation with focality that is still better than the exhaustive search (panels C2–C3 vs. A2–A3). Note that limiting the number of electrodes does not significantly add the computation time.

IV. Discussion

This paper compares two different methods that are recently proposed for optimizing the focality of IFS at one deep brain target on three MRI-derived realistic head models. We found that exhaustive search [2] on two pairs of electrodes is computationally intensive (takes $\sim$2 days) but gives more focal solution compared to rigorous optimization [1] when only 4 electrodes are available. The rigorous optimization is much faster ($\sim$6 hours) and is better in terms of focality but needs at least 8 electrodes. Therefore, we give the following guidelines:

- When only 4 electrodes are available, one should use the exhaustive search [2] and expect longer computation time;
- When more than 8 electrodes are available, one should use the rigorous optimization [1] for better focality. The rigorous optimization should start with the full array of 72 electrodes and be initialized using the solution from conventional high-definition transcranial electrical stimulation [15]. One should run the optimization for different levels of power constraint and finally choose the result with the best focality.

Future computational work will test the guidelines above on more targets, other directions of modulation, and across more head models. Other advanced algorithms for limiting the number of electrodes, such as branching-and-bound [16], could be considered. However, it may also increase the computational load. We note that since quasi-static field approximation implies linearity of the induced electric field, 4 mA total current stimulation will induce 2 times the electric field induced at 2 mA. This is especially relevant as the application of higher total current intensities (4 mA) for low intensity transcranial electrical stimulation research has been recently validated [17].

References

[1] Y. Huang, A. Datta, and L. C. Parra, "Optimization of interferential stimulation of the human brain with electrode arrays," *Journal of Neural Engineering*, vol. 17, no. 3, p. 036023, Jun. 2020, publisher: IOP Publishing. [Online]. Available: https://doi.org/10.1088%2F1741-2552%2Fab92b3

[2] S. Lee, C. Lee, J. Park, and C.-H. Im, "Individually customized transcranial temporal interference stimulation for focused modulation of deep brain structures: a simulation study with different head models," *Scientific Reports*, vol. 10, no. 1, p. 11730, Jul. 2020, number: 1 Publisher: Nature Publishing Group. [Online]. Available: https://www.nature.com/articles/s41598-020-68660-5

[3] N. Grossman, D. Bono, N. Dedic, S. B. Kodandaramaiah, A. Rudenko, H.-J. Suk, A. M. Cassara, E. Neufeld, N. Kuster, L.-H. Tsai *et al.*, "Noninvasive deep brain stimulation via temporally interfering electric fields," *Cell*, vol. 169, no. 6, pp. 1029–1041, 2017.

[4] Y. Huang and L. C. Parra, "Can transcranial electric stimulation with multiple electrodes reach deep targets?" *Brain Stimulation*, vol. 12, no. 1, pp. 30 – 40, 2019.

[5] S. Rampersad, B. Roig-Solvas, M. Yarossi, P. P. Kulkarni, E. Santarnecchi, A. D. Dorval, and D. H. Brooks, "Prospects for transcranial temporal interference stimulation in humans: a computational study," *bioRxiv*, 2019. [Online]. Available: https://www.biorxiv.org/content/early/2019/06/19/602102

[6] Q. Xiao, Z. Zhong, X. Lai, and H. Qin, "A multiple modulation synthesis method with high spatial resolution for noninvasive neurostimulation," *PLOS ONE*, vol. 14, no. 6, pp. 1–15, 06 2019. [Online]. Available: https://doi.org/10.1371/journal.pone.0218293

[7] Y. Huang, J. P. Dmochowski, Y. Su, A. Datta, C. Rorden, and L. C. Parra, "Automated MRI segmentation for individualized modeling of current flow in the human head," *Journal of Neural Engineering*, vol. 10, no. 6, p. 066004, Dec. 2013.

[8] S. Rush and D. A. Driscoll, "EEG electrode sensitivity–an application of reciprocity," *IEEE transactions on bio-medical engineering*, vol. 16, no. 1, pp. 15–22, Jan. 1969.

[9] J. P. Dmochowski, L. Koessler, A. M. Norcia, M. Bikson, and L. C. Parra, "Optimal use of eeg recordings to target active brain areas with transcranial electrical stimulation," *NeuroImage*, 2017.

[10] Y. Huang, A. Datta, M. Bikson, and L. C. Parra, "Realistic volumetric-approach to simulate transcranial electric stimulation—ROAST—a fully automated open-source pipeline," *Journal of Neural Engineering*, vol. 16, no. 5, p. 056006, Jul. 2019, publisher: IOP Publishing. [Online]. Available: https://doi.org/10.1088%2F1741-2552%2Fab208d

[11] Y. Huang, "Roast github repository," Jun. 2020, original-date: 2017-11-15T23:03:37Z. [Online]. Available: https://github.com/andypotatohy/roast

[12] G. H. Klem, H. O. Lüders, H. H. Jasper, and C. Elger, "The ten-twenty electrode system of the International Federation. The International Federation of Clinical Neurophysiology," *Electroencephalography and clinical neurophysiology. Supplement*, vol. 52, pp. 3–6, 1999.

[13] M. Fernández-Corazza, S. Turovets, and C. H. Muravchik, "Unification of optimal targeting methods in transcranial electrical stimulation," *NeuroImage*, vol. 209, p. 116403, 2020. [Online]. Available: https://www.sciencedirect.com/science/article/pii/S1053811919309942

[14] J. P. Dmochowski, M. Bikson, and L. C. Parra, "The point spread function of the human head and its implications for transcranial current stimulation," *Physics in medicine and biology*, vol. 57, no. 20, pp. 6459–6477, Oct. 2012.

[15] J. P. Dmochowski, A. Datta, M. Bikson, Y. Su, and L. C. Parra, "Optimized multi-electrode stimulation increases focality and intensity at target," *Journal of Neural Engineering*, vol. 8, no. 4, p. 046011, Aug. 2011.

[16] S. Boyd and J. Mattingley, "Branch and bound methods, notes for ee364b," 2007.

[17] C. D. Workman, J. Kamholz, and T. Rudroff, "Increased leg muscle fatigability during 2 mA and 4 mA transcranial direct current stimulation over the left motor cortex," *Experimental Brain Research*, vol. 238, no. 2, pp. 333–343, Feb. 2020.